Print ISSN : 0022-2755
Journal of Mines, Metals and Fuels
Contents available at: www.informaticsjournals.com/index.php/jmmf

Repercussions of Local Thermal Non-Equilibrium in Conjunction with Uniform/Non-uniform Thermal Gradients and Magnetic Flux on the Onset of Darcy-Rayleigh-Benard- Marangoni Convection in a Composite Layer

R. Sumithra[1] and Shyamala Venkatraman[2*]

[1]Associate Professor and 2Research Scholar, Department of UG, PG Studies & Research in Mathematics, Government Science College Autonomous, Nrupathunga University, Bengaluru, Karnataka, India. e-mail: sumitra_diya@yahoo.com and svr02009@gmail.com

Abstract

Repercussions of uniform/non-uniform thermal gradients such as linear, parabolic, inverted parabolic, piecewise linear gradient heated from below (PLHB), piecewise linear gradient cooled from above (PLCA) and step function (SF) thermal gradients in conjunction with magnetic flux on the onset of Darcy-Rayleigh-Benard-Marangoni (DRBMM) convection in a composite layer involving incompressible fluid and holding horizontal adiabatic boundaries, rigid beneath the porous layer and free aloft the fluid layer is performed apropos to Local Thermal Non-Equilibrium (LTNE). Regular Perturbation method is exercised to attain the analytical solution of the acquired problem. For all the six thermal gradients, (i) The strength of variables such as solid phase thermal expansion ratio, solid phase thermal diffusivity ratio and inter-phase thermal diffusivity ratio that boosts LTNE are analysed and (ii) The influence of change in measure of physical quantities viz. fluid phase thermal expansion ratio, fluid phase thermal diffusivity ratio, Chandrasekhar number and Marangoni number are studied.

Keywords: *Local Thermal Non Equilibrium (LTNE), Composite layer, thermal gradients, Regular Perturbation Method, Marangoni convection*

Nomenclature:

English letters			
$\vec{q}_{fl} = (u_{fl}, v_{fl}, w_{fl})$	: velocity vector	K	: permeability
t	: time	C_p	: specific heat capacity
P_{fl} & P_{po}	: pressure	Q_{fl}, Q_{po}	: Chandrasekhar numbers, defined below
g	: acceleration due to gravity		
T_{fl}, T_{fpo} & T_{spo}	: temperatures	h	: inter-phase heat transfer coefficient
T_0	: interface temperature		

*Corresponding author

English letters			
a_{fl} & a_{po}	: non dimensional horizontal wave numbers	H	: scaled inter-phase heat transfer coefficient
n_{fl} & n_{po}	: frequencies	$\hat{T}$	: thermal ratio
W_{fl} & W_{po}	: dimensionless vertical velocities	$\hat{d}$	: depth ratio
R_{fl}, R_{Tfpo}, R_{Tspo}	: Rayleigh numbers, defined below		
Greek Symbols			
ρ_0	: referrence density	κ_{FTD} & κ_{STD}	: thermal diffusivity ratio
μ_{fl}	: fluid viscosity	β	: porous parameter
ρ_{fl} & ρ_{po}	: fluid density	β^2	: Darcy number
κ_{fl}, κ_{fpo} & κ_{spo}	: thermal diffusivities	τ	: inter-phase thermal diffusivity ratio
α_{Tfl}, α_{Tfpo} & α_{Tspo}	: thermal expansion coefficients		
ϕ	: porosity	τ_{fpo} & τ_{mpo}	: diffusivity ratios
α_{FTE} & α_{STE}	: thermal expansion ratio	$\hat{\mu}$	: viscosity ratio
Subscripts			
fl	: fluid layer	s	: solid phase
po	: porous medium	b	: basic state
f	: fluid phase		

1. Introduction

The use of an electromagnetic field as a heat source is widely implemented in industrial processes such as heating, drying, melting, and pasteurizing. Transmission of heat through convection influenced by magnetic flux possess a significant place in appliances involving wellness activities, biophysics etc. Thermal equilibrium is assumed between solid porous matrix and saturated fluid in most of the available literatures related to thermal convection in porous media. But for sufficiently large Rayleigh number or rapid heat transfer for high speed flow, it can be expected that the equilibrium will break down, so that the respective local mean values of the temperature of solid and fluid phases are not same. Local thermal non-equilibrium (LTNE) state will be more suitable than local thermal equilibrium (LTE) state in this situation. Also, the assumption of LTE is inadmissible in many applications like air conditioner cooling, freezing of foods, microwave heating and in computer chips, so it has been significant to take account of the LTNE effects.

Barbosa [2005] analysed the challenge of improving phase change heat transfer prediction with respect to two phase non equilibrium models. Min Zeng and Qiuwang Wang [2009] examined natural convection with respect to diamagnetic fluid in a porous enclosure influenced by magnetic field. Sridhar Kulkarni [2013] examined unsteady heat convection in an anisotropic porous layer under rotation with respect to thermal non-equilibrium conditions. Armaghani et. al. [2017] investigated transfer of heat by forced convection with respect to nanofluids in a porous channel influenced by local thermal non-equilibrium using three models for thermal absorption. Ashoka [2017] analysed an algorithm based successive linearization method to obtain critical eigen value in a Rayleigh-Bénard-Brinkman Convection Problem including the boundary conditions. Mohsen et. al [2019] examined natural convection of nanofluid of hybrid nature and magnetisable, within a porous enclosure subjected to the effect of two variable magnetic fields. Sumithra and Manjunatha [2020] studied the impact of non-uniform temperature gradients on Darcian-Benard- Marangoni convection in the presence of Heat Source or Sink as well as Magnetic field with respect to composite layer

horizontally enclosed by adiabatic boundaries. Sumithra et. al. [2020] examined Benard-surface tension driven convection in an infinite horizontal composite layer in the presence of heat source/sink together with non-uniform temperature gradients influenced by magnetic field for non-Darcy model. Israa and Shatha [2021] studied the onset of convection with regard to bidispersive porous layer under anisotropy and influenced by local thermal non-equilibrium. Noura et.al. [2022] investigated mixed convection of an undulating cavity filled with nanofluid under local thermal non-equilibrium in the presence of obstacle and saturated by porous media.

Meagre research work has been carried out so far over composite layer considering LTNE into account. Inspired by the above survey of literature, the present paper examines the repercussions of uniform/non-uniform thermal gradients such as linear, parabolic, inverted parabolic, piecewise linear gradient heated from below (PLHB), piecewise linear gradient cooled from above (PLCA) and step function (SF) thermal gradients in conjunction with magnetic flux on the onset of Darcy-Rayleigh-Benard-Marangoni (DRBMM) convection in a composite layer involving incompressible fluid and holding horizontal adiabatic boundaries, rigid beneath the porous layer and free aloft the fluid layer under Local Thermal Non- Equilibrium (LTNE) conditions.

2. Mathematical formulation

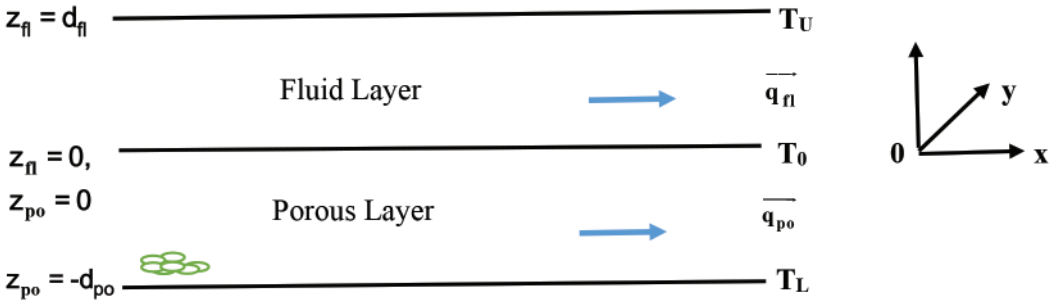

Figure 1: Prototypical Sketch

An infinite horizontal layer involving incompressible, Boussinesq electrically conducting fluid holding thickness $\mathbf{d_{fl}}$ is considered. Densely packed porous layer saturated with same fluid with thickness d_{po} lies beneath the fluid layer, and both the layers are levied with magnetic field of intensity H_0 in the perpendicular z-direction. The precinct below the porous layer is presumed to be rigid and that above the fluid layer is presumed to be with surface tension effects based on temperature. A Cartesian coordinate system in which the origin is placed at the interface between fluid and porous layers, and the z-axis pointing upright is considered. For the porous layer, solid phase as well as the fluid phase are purported to be in LTNE and a solid-fluid field model is considered to express distinctly the temperatures with regard to the solid and fluid phases. The above system is governed by the following basic equations.

$$\nabla.\vec{q}_{fl} = 0 \quad \text{... (1)}$$

$$\nabla.\overrightarrow{H_{fl}} = 0 \quad \text{... (2)}$$

$$\rho_0\left[\frac{\partial\vec{q}_{fl}}{\partial t} + \left(\vec{q}_{fl}.\nabla\right)\vec{q}_{fl}\right] = -\nabla P_{fl} + \mu\nabla^2\vec{q}_{fl} - \rho_{fl}g\hat{k} + \mu_p\left(\overrightarrow{H_{fl}}.\nabla\right)\overrightarrow{H_{fl}} \quad \text{... (3)}$$

$$\frac{\partial T_{fl}}{\partial t} + (\vec{q}_{fl}.\nabla)T_{fl} = \kappa_{fl}\nabla^2 T_{fl} \quad \text{... (4)}$$

$$\frac{\partial\overrightarrow{H_{fl}}}{\partial t} = \nabla\times q_{fl}\times\overrightarrow{H_{fl}} + \nu_m\nabla^2\overrightarrow{H_{fl}} \quad \text{... (5)}$$

$$\rho_{fl} = \rho_0[1-\alpha_{Tfl}(T_{fl}-T_0)] \quad \text{... (6)}$$

$$\nabla_m.\vec{q}_{po} = 0 \quad \text{... (7)}$$

$$\nabla_m . \overrightarrow{H_{fl}} = 0 \quad \text{... (8)}$$

$$\rho_0 \left[\frac{1}{\phi} \frac{\partial \vec{q}_{po}}{\partial t_{po}} + \frac{1}{\phi^2} (\vec{q}_{po} . \nabla_{po}) \vec{q}_{po} \right] = -\nabla_{po} P_{po} - \frac{\mu}{K} \vec{q}_{po} - \rho_{po} g \hat{k} + \mu_p \left(\overrightarrow{H_{fl}} . \nabla \right) \overrightarrow{H_{fl}} \quad \text{... (9)}$$

$$(\rho C_p)_{fpo} \left[\phi \frac{\partial T_{fpo}}{\partial t_{po}} + (\vec{q}_{po} . \nabla_{po}) T_{fpo} \right] = \phi \kappa_{fpo} \nabla_{po}^2 T_{fpo} + h(T_{spo} - T_{fpo}) \quad \text{... (10)}$$

$$(1-\phi)(\rho C_p)_{spo} \frac{\partial T_{spo}}{\partial t_{po}} = (1-\phi) \kappa_{spo} \nabla_{po}^2 T_{spo} - h(T_{spo} - T_{fpo}) \quad \text{... (11)}$$

$$\phi \frac{\partial \overrightarrow{H_{fl}}}{\partial t_{po}} = \nabla_{po} \times q_{po} \times \overrightarrow{H_{fl}} + \nu_{em} \nabla_{po}^2 \overrightarrow{H_{fl}} \quad \text{... (12)}$$

$$\rho_{po} = \rho_0 [1 - \alpha_{Tfpo} (T_{fpo} - T_0) - \alpha_{Tspo} (T_{spo} - T_0)] \quad \text{... (13)}$$

The system is quiescent for which the basic state is expressed by

$$[u_{fl}, v_{fl}, w_{fl}, P_{fl}, T_{fl}, \overrightarrow{H_{fl}}] = [0,0,0, P_{flb}(z_{fl}), T_{flb}(z_{fl}), H_0(z_{fl})] \text{ in the fluid layer} \quad \text{... (14)}$$

and $$[u_{po}, v_{po}, w_{po}, P_{po}, T_{fpo}, T_{spo}, \overrightarrow{H_{fl}}] = [0,0,0, P_{pob}(z_{po}), T_{fpob}(z_{po}), T_{spob}(z_{po}), H_0(z_{po})] \quad \text{... (15)}$$

in the porous layer

The basic state temperature distributions $T_{flb}(z_{fl})$, $T_{fpob}(z_{po})$ and $T_{spob}(z_{po})$ respectively are found to be

$$T_{flb}(z_{fl}) = T_0 - \frac{T_0 - T_U}{d_{fl}} z_{fl} \text{ in } 0 \le z_{fl} \le d_{fl} \quad \text{... (16)}$$

$$T_{fpob}(z_{po}) = T_0 - \frac{T_L - T_0}{d_{po}} z_{po} = T_{pob}(z_{po}) \text{ in } -d_{po} \le z_{po} \le 0 \quad \text{... (17)}$$

For investigating stability of the basic solution, following diminutive disturbances are introduced.

$$[\vec{q}_{fl}, P_{fl}, T_{fl}, \overrightarrow{H_{fl}}] = [0, P_{flb}(z_{fl}), T_{flb}(z_{fl}), H_0(z_{fl})] + [\vec{q}_{fl}', P_{fl}', \theta_{fl}, \overrightarrow{H_{fl}}'] \quad \text{... (18)}$$

$$[\vec{q}_{po}, P_{po}, T_{fpo}, T_{spo}, \overrightarrow{H_{fl}}] = [0, P_{pob}(z_{po}), T_{fpob}(z_{po}), T_{spob}(z_{po}), H_0(z_{po})] + [\vec{q}_{po}', P_{po}', \theta_{fpo}, \theta_{spo}, \overrightarrow{H_{fl}}'] \quad \text{... (19)}$$

where the prime indicates perturbation over the equilibrium counterparts. Now (18) and (19) are placed in the corresponding physical quantities of equations (1) to (13) and are linearized in the customary manner. Then, the pressure term is removed from (3) and (9) by the procedure of operating curl two times on these two equations and keeping only the vertical component.

Next, the resulting equations are nondimensionalised applying $d_{fl}, \frac{d_{fl}^2}{\kappa_{fl}}, \frac{\kappa_{fl}}{d_{fl}}, T_0 - T_U, H_0$ as the units of length, time, velocity, temperature and magnetic field in the fluid layer correspondingly and $\frac{d_{po}^2}{\kappa_{fpo}}, \frac{\kappa_{fpo}}{d_{po}}, T_L - T_0, H_0$ as the units of time, velocity and temperature in the porous layer whereas the scale for length in the porous layer is $(x_{po}, y_{po}, z_{po}) = d_{po}(x'_{po}, y'_{po}, z'_{po} - 1)$. Following this fashion, the flow- fields pertaining to fluid as well as porous layers can be achieved for all depth ratios $\hat{d} = \frac{d_{po}}{d_{fl}}$. Normal mode analysis is performed on the dimensionless equations as follows:

$$\begin{bmatrix} W_{fl} \\ \theta_{fl} \\ H_{fl} \end{bmatrix} = \begin{bmatrix} W_{fl}(z_{fl}) \\ \theta_{fl}(z_{fl}) \\ H_{fl}(z_{fl}) \end{bmatrix} f_{fl}(x_{fl}, y_{fl}) e^{n_{fl} t} \quad \text{... (20)}$$

$$\begin{bmatrix} W_{po} \\ \theta_{fpo} \\ \theta_{spo} \\ H_{fl} \end{bmatrix} = \begin{bmatrix} W_{po}(z_{po}) \\ \theta_{fpo}(z_{po}) \\ \theta_{spo}(z_{po}) \\ H_{fl}(z_{po}) \end{bmatrix} f_{po}(x_{po}, y_{po}) e^{n_{po} t} \quad \text{... (21)}$$

with $\nabla^2 f_{fl} + a_{fl}^2 f_{fl} = 0$ and $\nabla_{po}^2 f_{po} + a_{po}^2 f_{po} = 0$

The resulting equations are:

In $0 \le z_{fl} \le 1$

$$(D_{fl}^2 - a_{fl}^2)^2 W_{fl} = R_{fl} a_{fl}^2 \theta_{fl} + Q_{fl} D_{fl}^2 W_{fl} \quad \text{... (22)}$$

$$(D_{fl}^2 - a_{fl}^2)\theta_{fl} + W_{fl} = 0 \quad \text{... (23)}$$

In **$0 < z_{po} < 1$**

$$(D_{po}^2 - a_{po}^2)^2 W_{po} = -\beta^2 R_{Tfpo} a_{po}^2 \theta_{fpo} - \beta^2 R_{Tspo} a_{po}^2 \theta_{spo} \tau - Q_{po} \beta^2 D_{po}^2 W_{po} \quad \text{... (24)}$$

$$\phi(D_{po}^2 - a_{po}^2)\theta_{fpo} + W_{po} = -H(\theta_{spo} - \theta_{fpo}) \quad \text{... (25)}$$

$$(1-\phi)(D_{po}^2 - a_{po}^2)\theta_{spo} = H(\theta_{spo} - \theta_{fpo}) \quad \text{... (26)}$$

Where for the fluid layer, $R_{fl} = \dfrac{g\alpha_{Tfl}(T_0 - T_U) d_{fl}^3}{\nu_{fl}\kappa_{fl}}$ specifies the Rayleigh number, $Q_{fl} = \dfrac{\mu_p H_0^2 d_{fl}^2}{\mu_{fl}\kappa_{fl}\tau_{fpo}}$ specifies the Chandrasekhar number, $\tau_{fpo} = \dfrac{\nu_{pov}}{\kappa_{fl}}$ specifies the diffusivity ratio, and for the porous layer, $R_{Tfpo} = \dfrac{g\alpha_{Tfpo}(T_L - T_0) d_{po}^3}{\nu_{fl}\kappa_{fpo}}$ specifies the fluid Rayleigh number, $R_{Tspo} = \dfrac{g\alpha_{Tspo}(T_L - T_0) d_{po}^3}{\nu\kappa_{spo}}$ specifies the solid Rayleigh number, $\beta^2 = \dfrac{K}{d_{po}^2} = Da$ specifies the Darcy number, $Q_{po} = \dfrac{\mu_p H_0^2 d_{po}^2}{\mu_{fl}\kappa_{po}\tau_{mpo}} = Q_{fl}\varepsilon\hat{d}^2$ specifies the Chandrasekhar number, $\tau_{mpo} = \dfrac{\nu_{epo}}{\kappa_{po}}$ specifies the diffusivity ratio, $\tau = \dfrac{\kappa_{spo}}{\kappa_{fpo}}$ specifies the ratio of thermal diffusivity of the solid to the fluid phase, $H = \dfrac{h d_{po}^2}{\kappa_{fpo}}$ specifies the scaled inter-phase heat transfer coefficient.

Equations (22) to (26) are ordinary differential equations of fourteenth order and required to be solved with the help of the following fourteen boundary conditions.

3. Boundary conditions

Normal mode expansion performed on the appropriate boundary conditions after non dimensionalization. They are,

$$W_{fl}(1) = 0, \quad D_{fl}^2 W_{fl}(1) + M_{fl} a_{fl}^2 \theta_{fl}(1) = 0, \quad D_{fl}\theta_{fl}(1) = 0,$$

$$\hat{T} W_{fl}(0) = W_{po}(1), \quad \hat{T}\hat{d} D_{fl} W_{fl}(0) = \hat{\mu} D_{po} W_{po}(1)$$

$$\theta_{fl}(0) = \hat{T}\theta_{fpo}(1), \quad \theta_{fl}(0) = \hat{T}\theta_{spo}(1), \quad D_{fl}\theta_{fl}(0) = D_{po}\theta_{fpo}(1), \quad D_{fl}\theta_{fl}(0) = D_{po}\theta_{spo}(1)$$

$$\hat{T}\hat{d}^3\beta^2[D_{fl}^3 W_{fl}(0) - 3a_{fl}^2 D_{fl} W_{fl}(0)] = -D_{po} W_{po}(1) + \hat{\mu}\beta^2[D_{po}^3 W_{po}(1) - 3a_{po}^2 D_{po} W_{po}(1)]$$

$$\hat{T}\hat{d}^2(D_{fl}^2 + a_{fl}^2) W_{fl}(0) = \hat{\mu}(D_{po}^2 + a_{po}^2) W_{po}(1)$$

$$W_{po}(0) = 0, \quad D_{po} W_{po}(0) = 0, \quad D_{po}\theta_{fpo}(0) = 0, \quad D_{po}\theta_{spo}(0) = 0$$

Where $\hat{T} = \frac{T_L - T_0}{T_0 - T_U}$ specifies the thermal ratio, $\beta = \sqrt{\frac{K}{d_{po}^2}}$, $\hat{d} = \frac{d_{po}}{d_{fl}}$ specifies the depth ratio and $\hat{\mu} = \frac{\mu_{po}}{\mu_{fl}}$ specifies the viscosity ratio.

4. Solving using regular perturbation method

At boundaries with constant heat dissipation, convection occurs for smaller horizontal wave number 'a fl '. Hence we expand

$$\begin{bmatrix} W_{fl} \\ \theta_{fl} \end{bmatrix} = \sum_{j=0}^{\infty} a_{fl}^{2j} \begin{bmatrix} W_{flj} \\ \theta_{flj} \end{bmatrix} \text{ and } \begin{bmatrix} W_{po} \\ \theta_{fpo} \\ \theta_{spo} \end{bmatrix} = \sum_{j=0}^{\infty} a_{po}^{2j} \begin{bmatrix} W_{poj} \\ \theta_{fpoj} \\ \theta_{spoj} \end{bmatrix}$$

Zero order system is solved using an arbitrary factor and the solutions are

$W_{fl0}(z_{fl}) = 0$, $\theta_{fl0}(z_{fl}) = \hat{T}$, $W_{po0}(z_{po}) = 0$, $\theta_{fpo0}(z_{po}) = 1$, $\theta_{spo0}(z_{po}) = 1$

The first order equations in a_{fl}^2 are:

For fluid layer,

$$D_{fl}^4 W_{fl1} - R_{fl}\hat{T} - Q_{fl} D_{fl}^2 W_{fl1} = 0 \quad \text{... (27)}$$

$$D_{fl}^2 \theta_{fl1} - \hat{T} + W_{fl1} = 0 \quad \text{... (28)}$$

For porous layer,

$$D_{po}^2 W_{po1} + Q_{po}\beta^2 D_{po}^2 W_{po1} + \beta^2 R_{Tfpo} + \beta^2 R_{Tspo}\tau = 0 \quad \text{... (29)}$$

$$(\phi D_{po}^2 - H)\theta_{fpo1} + H\theta_{spo1} + W_{po1} - \phi = 0 \quad \text{... (30)}$$

$$[(1-\phi)D_{po}^2 - H]\theta_{spo1} + H\theta_{fpo1} - (1-\phi) = 0 \quad \text{... (31)}$$

The corresponding boundary conditions are

$W_{fl1}(1) = 0$, $D_{fl}^2 W_{fl1}(1) + M_{fl}\theta_{fl0}(1) = 0$, $D_{fl}\theta_{fl1}(1) = 0$

$\hat{T} W_{fl1}(0) = \hat{d}^2 W_{po1}(1)$, $\hat{T} D_{fl} W_{fl1}(0) = \hat{\mu}\hat{d} D_{po} W_{po1}(1)$

$\theta_{fl1}(0) = \hat{T}\hat{d}^2 \theta_{fpo1}(1)$, $\theta_{fl1}(0) = \hat{T}\hat{d}^2 \theta_{spo1}(1)$

$D_{fl}\theta_{fl1}(0) = \hat{d}^2 D_{po}\theta_{fpo1}(1)$, $D_{fl}\theta_{fl1}(0) = \hat{d}^2 D_{po}\theta_{spo1}(1)$

$\hat{T}\hat{d}\beta^2 D_{fl}^3 W_{fl1}(0) = -D_{po} W_{po1}(1) + \hat{\mu}\beta^2 D_{po}^3 W_{po1}(1)$, $\hat{T} D_{fl}^2 W_{fl1}(0) = \hat{\mu} D_{po}^2 W_{po1}(1)$

$W_{po1}(0) = 0$, $D_{po} W_{po1}(0) = 0$, $D_{po}\theta_{fpo1}(0) = 0$, $D_{po}\theta_{spo1}(0) = 0$

W_{fl1} and W_{po1} are obtained by solving equations (27) & (29) and are

$$W_{fl1}(z) = C_1 + C_2 z_{fl} + C_3 \text{Cosh}\sqrt{Q_{fl}} z_{fl} + C_4 \text{Sinh}\sqrt{Q}_{fl} z_{fl} - \frac{R_{fl}\hat{T}}{2Q_{fl}} z_{fl}^2 \quad \text{... (32)}$$

$$W_{po1}(z_{po}) = C_5 + C_6 z_{po} - \frac{\beta^2 R_{Tfpo} + \beta^2 R_{Tspo}\tau}{2(1 + Q_{po}\beta^2)} z_{po}^2 \quad \text{... (33)}$$

Where the constants C_1, C_2, C_3, C_4, C_5 & C_6 evaluated using velocity boundary conditions, are

$$C_1 = \frac{R_{Tfpo} + R_{Tspo}\tau}{\hat{T}(1 + Q_{po}\beta^2)}\left[\frac{1}{\hat{d}Q_{fl}} + \hat{\mu}\hat{d}\beta^2\right] - \frac{R_{fl}\hat{T}}{Q_{fl}^2} + \frac{M_{fl}\hat{T}}{Q_{fl}^2} + \frac{R_{fl}\hat{T}}{2Q_{fl}}, \quad C_2 = \frac{-(R_{Tfpo} + R_{Tspo}\tau)}{\hat{T}(1 + Q_{po}\beta^2)}\left[\frac{1}{\hat{d}Q_{fl}} + \hat{\mu}\hat{d}\beta^2\right],$$

$$C_3 = \frac{R_{fl}\hat{T}}{{Q_{fl}}^2 \operatorname{Cosh}\sqrt{Q_{fl}}} - \frac{M_{fl}\hat{T}}{Q_{fl}\operatorname{Cosh}\sqrt{Q_{fl}}} - \frac{\operatorname{Tanh}\sqrt{Q_{fl}}}{\hat{T}\hat{d}Q_{fl}\sqrt{Q_{fl}}}.\frac{(R_{Tfpo}+R_{Tspo}\tau)}{1+Q_{po}\beta^2},$$

$$C_4 = \frac{R_{Tfpo}+R_{Tspo}\tau}{1+Q_{po}\beta^2}.\frac{1}{\hat{T}\hat{d}Q_{fl}\sqrt{Q_{fl}}}, \quad C_5 = C_6 = 0$$

4.1 Solvability Condition:

The compatibility condition derived from the differential equations and boundary conditions with respect to temperature is

$$\int_0^1 W_{fl1}(z_{fl})G_{fl}(z_{fl})dz_{fl} + \hat{d}^2\int_0^1 W_{po1}(z_{po})G_{po}(z_{po})dz_{po} = \hat{d}^2 + \hat{T} \quad \text{... (34)}$$

$W_{fl1}(z_{fl})\,\&\,W_{po1}(z_{po})$ are substituted in equation (34) and Critical Rayleigh Number is obtained for distinct basic thermal profiles with respect to fluid as well as porous layers.

4.2. Linear Thermal Gradient:

For this gradient, $G_{fl}(z_{fl}) = G_{po}(z_{po}) = 1$ ... (35)

For this model, the critical Rayleigh number is achieved by using (35) in (34) and is calculated as

$$R_{CL} = \frac{\hat{d}^2 + \hat{T} - \delta_8}{-\delta_1 + \delta_2 + \delta_3 + \left[\alpha_{FTE}{\kappa_{FTD}}^2 + \alpha_{STE}{\kappa_{STD}}^2\tau\right]\hat{d}^4\Delta_1\left(\delta_4 + \delta_5 - \delta_6 - \delta_7\right)}$$

where $\delta_1 = \frac{\hat{T}}{{Q_{fl}}^2}$, $\delta_2 = \frac{\hat{T}}{{Q_{fl}}^2\sqrt{Q_{fl}}}\operatorname{Tanh}\sqrt{Q_{fl}}$, $\delta_3 = \frac{\hat{T}}{3Q_{fl}}$, $\delta_4 = \frac{1}{2\hat{T}}\left(\frac{1}{\hat{d}Q_{fl}} + \hat{\mu}\hat{d}\beta^2\right)$,

$$\delta_5 = \frac{1}{\hat{T}\hat{d}Q_{fl}\sqrt{Q_{fl}}}\left[\operatorname{Sinh}\sqrt{Q_{fl}} - \frac{1}{\sqrt{Q_{fl}}}\left(\operatorname{Sech}\sqrt{Q_{fl}} - \operatorname{Cosh}\sqrt{Q_{fl}}\right)\right],$$

$$\delta_6 = \frac{1}{\hat{T}\hat{d}Q_{fl}\sqrt{Q_{fl}}}\left[\operatorname{Sinh}\sqrt{Q_{fl}} - \frac{\operatorname{Cosh}\sqrt{Q_{fl}}}{\sqrt{Q_{fl}}} + \frac{1}{Q_{fl}}\right], \quad \delta_7 = \frac{\hat{d}^2\beta^2}{6}, \quad \delta_8 = \frac{M_{fl}\hat{T}}{Q_{fl}}\left(1 - \frac{\operatorname{Tanh}\sqrt{Q_{fl}}}{\sqrt{Q_{fl}}}\right),$$

$\Delta_1 = \frac{1}{1+Q_m\beta^2}$ and $\alpha_{FTE} = \frac{\alpha_{Tfpo}}{\alpha_{Tfl}}$ is the ratio of the thermal expansion coefficients of fluid phase in porous layer to the thermal expansion coefficient in the fluid layer, $\alpha_{STE} = \frac{\alpha_{Tspo}}{\alpha_{Tfl}}$ represents ratio of the thermal expansion coefficient of solid phase in porous layer to the thermal expansion coefficient in the fluid layer, $\kappa_{FTD} = \frac{\kappa_{fl}}{\kappa_{fpo}}$ represents ratio of thermal diffusivity in fluid layer to that of fluid phase in the porous layer, $\kappa_{STD} = \frac{\kappa_{fl}}{\kappa_{spo}}$ is the ratio of thermal diffusivity in fluid layer to that of solid phase in the porous layer.

4.3. Parabolic Thermal Gradient:

Here, $G_{fl}(z_{fl}) = 2z_{fl}\ \&\ G_{po}(z_{po}) = 2z_{po}$ ... (36)

For this model, the critical Rayleigh number is achieved by using (36) in (34) and is calculated as

$$R_{CP} = \frac{\hat{d}^2 + \hat{T} + B_{12}\left(B_2 + B_3\right)}{B_1\left(B_2 + B_3\right) + B_4 + \left[\alpha_{FTE}\kappa_{FTD}{}^2 + \alpha_{STE}\kappa_{STD}{}^2\tau\right]\hat{d}^4 B_5\left\{B_6 - B_7\left(B_2 + B_3\right) + B_8\left(B_9 + B_{10}\right) - B_{11}\right\}}$$

where $B_1 = \frac{\hat{T}}{Q_{fl}{}^2\,\mathrm{Cosh}\sqrt{Q_{fl}}}$, $B_2 = -\mathrm{Cosh}\sqrt{Q_{fl}}\left(1 + \frac{2}{Q_{fl}}\right)$, $B_3 = \frac{2}{\sqrt{Q_{fl}}}\left(\mathrm{Sinh}\sqrt{Q_{fl}} + \frac{1}{\sqrt{Q_{fl}}}\right)$,

$B_4 = \frac{\hat{T}}{4Q_{fl}}$, $B_5 = \frac{1}{1 + Q_{po}\beta^2}$, $B_6 = \frac{1}{3\hat{T}}\left(\frac{1}{\hat{d}Q_{fl}} + \hat{\mu}\hat{d}\beta^2\right)$, $B_7 = \frac{\mathrm{Tanh}\sqrt{Q_{fl}}}{\hat{T}\hat{d}Q_{fl}\sqrt{Q_{fl}}}$, $B_8 = \frac{1}{\hat{T}\hat{d}Q_{fl}\sqrt{Q_{fl}}}$,

$B_9 = -\mathrm{Sinh}\sqrt{Q_{fl}}\left(1 + \frac{2}{Q_{fl}}\right)$, $B_{10} = \frac{2}{\sqrt{Q_{fl}}}\mathrm{Cosh}\sqrt{Q_{fl}}$, $B_{11} = \frac{\hat{d}^2\beta^2}{4}$, $B_{12} = \frac{M\hat{T}}{Q_{fl}\,\mathrm{Cosh}\sqrt{Q_{fl}}}$

And α_{FTE}, α_{STE}, κ_{FTD} and κ_{STD} remain the same as above.

4.4. Inverted Parabolic Thermal Gradient:

Here, $G_{fl}(z_{fl}) = 2(1 - z_{fl})$ & $G_{po}(z_{po}) = 2(1 - z_{po})$ ... (37)

For this model, the critical Rayleigh number is achieved by using (37) in (34) and is calculated as

$$R_{CIP} = \frac{\hat{d}^2 + \hat{T} - 2\delta_8 - B_{12}\left(B_2 + B_3\right)}{\delta_{11} + B_{13} + \left[\alpha_{FTE}\kappa_{FTD}{}^2 + \alpha_{STE}\kappa_{STD}{}^2\tau\right]\hat{d}^4\left\{\Delta_1\right\}\left(\delta_{12} - B_{14}\right)}$$

where

$\delta_{11} = -2\delta_1 + 2\delta_2 - 2\delta_3$

$B_{13} = -B_1\left(B_2 + B_3\right) - B_4$

$\delta_{12} = 2\delta_4 + 2\delta_5 - 2\delta_6 - 2\delta_7$

$B_{14} = B_5\left[B_6 - B_7\left(B_2 + B_3\right) + B_8\left(B_9 + B_{10}\right) - B_{11}\right]$

And α_{FTE}, α_{STE}, κ_{FTD} and κ_{STD},
B_1, B_2, B_3, B_4, B_5, B_6, B_7, B_8, B_9, B_{10}, B_{11}, B_{12}, δ_1, δ_2, δ_3, δ_4, δ_5, δ_6, δ_7 & δ_8 remain the same as above.

4.5. Piecewise Linear Gradient Heated from Below:

In this case, $G_{fl}(z_{fl}) = \begin{cases} \varepsilon_{fl}^{-1}, 0 \le z_{fl} \le \varepsilon_{fl} \\ 0 \quad , \varepsilon_{fl} \le z_{fl} \le 1 \end{cases}$ and $G_{po}(z_{po}) = \begin{cases} \varepsilon_{po}^{-1}, 0 \le z_{po} \le \varepsilon_{po} \\ 0 \quad , \varepsilon_{po} \le z_{po} \le 1 \end{cases}$ ... (38)

For this model, the critical Rayleigh number is achieved by using (38) in (24) and is calculated as

$$R_{CHFB} = \frac{\hat{d}^2 + \hat{T} + D_{13}\left(-\mathrm{Cosh}\sqrt{Q_{fl}} + D_2\right)}{D_1\left(-\mathrm{Cosh}\sqrt{Q_{fl}} + D_2\right) + D_3 - D_4 + \left[\alpha_{FTE}\kappa_{FTD}{}^2 + \alpha_{STE}\kappa_{STD}{}^2\tau\right]\hat{d}^4 D_5.D_{14}}$$

Where $D_{14} = D_6.D_7 - D_8\left(-\mathrm{Cosh}\sqrt{Q_{fl}} + D_2\right) + D_9\left(-\mathrm{Sinh}\sqrt{Q_{fl}} + D_{10} - D_{11}\right) - D_{12}$ and

$D_1 = \frac{\hat{T}}{Q_{fl}{}^2\,\mathrm{Cosh}\sqrt{Q_{fl}}}$, $D_2 = \frac{\mathrm{Sinh}\left[\sqrt{Q_{fl}}\varepsilon_{fl}\right]}{\varepsilon\sqrt{Q_{fl}}}$, $D_3 = \frac{\hat{T}}{2Q_{fl}}$, $D_4 = \frac{\hat{T}\varepsilon_{fl}{}^2}{6Q_{fl}}$, $D_5 = \frac{1}{1 + Q_{po}\beta^2}$,

$D_6 = \frac{1}{\hat{T}}\left(\frac{1}{\hat{d}Q_{fl}} + \hat{\mu}\hat{d}\beta^2\right)$, $D_7 = -1 + \frac{\varepsilon_{fl}}{2}$, $D_8 = \frac{\mathrm{Tanh}\sqrt{Q_{fl}}}{\hat{T}\hat{d}Q_{fl}\sqrt{Q_{fl}}}$, $D_9 = \frac{1}{\hat{T}\hat{d}Q_{fl}\sqrt{Q_{fl}}}$,

$D_{10} = \frac{1}{\varepsilon_{fl}\sqrt{Q_{fl}}}\mathrm{Cosh}\left[\sqrt{Q_{fl}}\varepsilon_{fl}\right]$, $D_{11} = \frac{1}{\varepsilon_{fl}\sqrt{Q_{fl}}}$, $D_{12} = \frac{\hat{d}^2\beta^2}{6}\varepsilon_{po}{}^2$, $D_{13} = \frac{M\hat{T}}{Q_{fl}\,\mathrm{Cosh}\sqrt{Q_{fl}}}$

And α_{FTE}, α_{STE}, κ_{FTD} and κ_{STD} remain the same as above.

4.6. Piecewise Linear Gradient Cooled from Above:

In this case,

$$G_{fl}(z_{fl}) = \begin{cases} 0 & ,0 \le z_{fl} \le (1-\varepsilon_{fl}) \\ \varepsilon_{fl}^{-1}, & (1-\varepsilon_{fl}) \le z_{fl} \le 1 \end{cases} \text{ and } G_{po}(z_{po}) = \begin{cases} 0 & ,0 \le z_{po} \le (1-\varepsilon_{po}) \\ \varepsilon_{po}^{-1} & ,(1-\varepsilon_{po}) \le z_{po} \le 1 \end{cases} \quad \text{... (39)}$$

For this model, the critical Rayleigh number is achieved by using (39) in (34) and is calculated as

$$R_{CCFA} = \frac{\hat{d}^2 + \hat{T} + G_{12}\left(-\mathrm{Cosh}\sqrt{Q_{fl}} + G_2\right)}{G_1\left(-\mathrm{Cosh}\sqrt{Q_{fl}} + G_2\right) + G_3 - G_4 + \left[\alpha_{FTE}{\kappa_{FTD}}^2 + \alpha_{STE}{\kappa_{STD}}^2\tau\right]\hat{d}^4 G_5.G_{14}}$$

Where $G_{14} = G_6.G_7 - G_8\left(-\mathrm{Cosh}\sqrt{Q_{fl}} + G_2\right) + G_9\left(-\mathrm{Sinh}\sqrt{Q_{fl}} + G_{10} - G_{11}\right)$ and

$$G_1 = \frac{\hat{T}}{{Q_{fl}}^2\,\mathrm{Cosh}\sqrt{Q_{fl}}},\ G_2 = \frac{\mathrm{Sinh}\sqrt{Q_{fl}} - \mathrm{Sinh}\left\{\sqrt{Q_{fl}}\left(1-\varepsilon_{fl}\right)\right\}}{\varepsilon_{fl}\sqrt{Q_{fl}}},\ G_3 = \frac{\hat{T}}{2Q_{fl}},\ G_4 = \frac{\hat{T}\left[1-\left(1-\varepsilon_{fl}\right)^3\right]}{6Q_{fl}\varepsilon_{fl}},$$

$$G_5 = \frac{1}{1+Q_{po}\beta^2},\ G_6 = \frac{-1}{\hat{T}}\left(\frac{1}{\hat{d}Q_{fl}} + \hat{\mu}\hat{d}\beta^2\right),\ G_7 = -1 + \frac{1-(1-\varepsilon_{fl})^2}{2\varepsilon_{fl}},\ G_8 = \frac{\mathrm{Tanh}\sqrt{Q_{fl}}}{\hat{T}\hat{d}Q_{fl}\sqrt{Q_{fl}}},\ G_9 = \frac{1}{\hat{T}\hat{d}Q_{fl}\sqrt{Q_{fl}}},$$

$$G_{10} = \frac{\mathrm{Cosh}\sqrt{Q_{fl}} - \mathrm{Cosh}\left\{\sqrt{Q_{fl}}\left(1-\varepsilon_{fl}\right)\right\}}{\varepsilon_{fl}\sqrt{Q_{fl}}},\ G_{11} = \frac{\hat{d}^2\beta^2}{6\varepsilon_{po}}\left[1-\left(1-\varepsilon_{po}\right)^3\right],\ G_{12} = \frac{M\hat{T}}{Q_{fl}\,\mathrm{Cosh}\sqrt{Q_{fl}}}$$

And α_{FTE}, α_{STE}, κ_{FTD} and κ_{STD} remain the same as above.

4.7. Step Function Thermal Gradient:

In this gradient the basic temperature falls suddenly by an amount ΔT_{fl} at $z_{fl} = \varepsilon_{fl}$ and ΔT_{po} $z_{po} = \varepsilon_{po}$ otherwise uniform. Accordingly,

$$G_{fl}(z_{fl}) = \delta(z_{fl} - \varepsilon_{fl})\ \&\ G_{po}(z_{po}) = \delta(z_{po} - \varepsilon_{po}) \quad \text{... (40)}$$

For this model, the critical Rayleigh number is achieved by using (40) in (34) and is calculated as

$$R_{CSF} = \frac{\hat{d}^2 + \hat{T} + J_{12}.J_2}{J_1.J_2 + J_3 - J_4 + \left[\alpha_{FTE}{\kappa_{FTD}}^2 + \alpha_{STE}{\kappa_{STD}}^2\tau\right]\hat{d}^4 J_5\left(J_6.J_7 - J_8.J_2 + J_9.J_{10} - J_{11}\right)}$$

where $J_1 = \frac{\hat{T}}{{Q_{fl}}^2\,\mathrm{Cosh}\sqrt{Q_{fl}}},\ J_2 = -\mathrm{Cosh}\sqrt{Q_{fl}} + \mathrm{Cosh}\left[\sqrt{Q_{fl}}\varepsilon_{fl}\right],\ J_3 = \frac{\hat{T}}{2Q_{fl}},\ J_4 = \frac{\hat{T}{\varepsilon_{fl}}^2}{2Q_{fl}},$

$$J_5 = \frac{1}{1+Q_{po}\beta^2},\ J_6 = \frac{-1}{\hat{T}}\left(\frac{1}{\hat{d}Q_{fl}} + \hat{\mu}\hat{d}\beta^2\right),\ J_7 = -1 + \varepsilon_{fl},\ J_8 = \frac{\mathrm{Tanh}\sqrt{Q_{fl}}}{\hat{T}\hat{d}Q_{fl}\sqrt{Q_{fl}}},\ J_9 = \frac{1}{\hat{T}\hat{d}Q_{fl}\sqrt{Q_{fl}}},$$

$$J_{10} = -\mathrm{Sinh}\sqrt{Q_{fl}} + \mathrm{Sinh}\left[\sqrt{Q_{fl}}\varepsilon_{fl}\right],\ J_{11} = \frac{\hat{d}^2\beta^2}{2}{\varepsilon_{po}}^2,\ J_{12} = \frac{M\hat{T}}{Q_{fl}\,\mathrm{Cosh}\sqrt{Q_{fl}}},$$

5. Results and Discussions

Repercussions of uniform/non-uniform thermal gradients namely linear, parabolic, inverted parabolic, piecewise linear heated from below (PLHB), piecewise linear cooled from above (PLCA) and step function (SF) thermal gradient influenced by magnetic flux are analysed with respect to LTNE model on DRBMM convection in

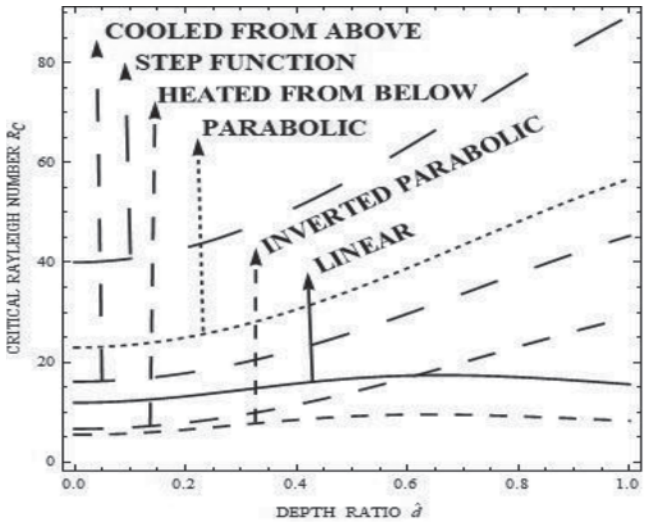

Figure-2: Comparison-Critical Rayleigh Number (RC) for 6 gradients with respect to LTNE model

composite layer.

Graphical interpretation for critical Rayleigh number R_C versus depth ratio $\hat{d}$ for the fixed values of $\alpha_{STE} = 2$, $\kappa_{STD} = 0.5$, $\tau = 0.1$, $\alpha_{FTE} = 1$, $\kappa_{FTD} = 0.4$, $Q_{fl} = 10$ and $M_{fl} = 10$ has been exposed with regard to linear, parabolic, inverted parabolic, PLHB, PLCA and SF thermal gradients in case of rigid free boundaries. The SF thermal gradient is profoundly stable whereas the inverted parabolic thermal gradient is remarkably unstable.

The result on varying each of the variables namely solid phase thermal expansion ratio α_{STE}, solid phase thermal diffusivity ratio κ_{STD}, inter-phase diffusivity ratio τ, fluid phase thermal expansion ratio α_{FTE}, fluid phase thermal diffusivity ratio κ_{FTD}, Chandrasekhar number Q_{fl} and Marangoni number M_{fl} on critical Rayleigh number keeping the remaining parameters unaltered are illustrated with regard to LTNE conditions via figures (3.1), (4.1), (5.1), (6.1), (7.1), (8.1) and (9.1) respectively for linear, parabolic and inverted parabolic thermal gradients and via figures (3.2), (4.2), (5.2), (6.2), (7.2), (8.2), and (9.2) respectively for piecewise linear gradient heated from below, piecewise linear gradient cooled from above and step function thermal gradients.

The effects of solid phase thermal expansion ratio α_{STE} over critical Rayleigh number are represented in figures 3.1and 3.2 considering $\alpha_{STE} = 2$, 6 and 10. The curves are found diverging thereby witnessing the effect of this parameter for porous layer dominant composite system. The system gets destabilized since the critical Rayleigh number diminishes with an augmentation of α_{STE}. The control of DRBMM convection effusively dependent on the thermal expansion of the solid phase with respect to all the six gradients. Lesser the thermal expansion of the solid phase, better is the control of DRBMM convection. It is observed from the graph that parabolic thermal gradient is most stable whereas inverted parabolic thermal gradient is most unstable and PLHB is most unstable whereas SF is most stable. The effect of the parameter is very less for inverted parabolic gradient and higher for parabolic gradient the whereas the effect of the parameter is very less in case of PLHB gradient and higher in case of SF temperature gradient.

The influence of solid phase thermal diffusivity ratio κ_{STD} over critical Rayleigh number are depicted in figures 4.1 and 4.2 when $\kappa_{STD} = 0.1$, 0.5 and 0.9. Divergence is noticed from the figure and is evident that it is sensitive in composite layers dominated by porous layer. Also, decline in critical Rayleigh number is noticed when κ_{STD} rises which destabilizes the system. Hence, preponement of onset of DRBMM convection, is observed. DRBMM convection is better controlled for smaller values of thermal difusivity of the solid phase.The graphs show that parabolic thermal gradient is most stable whereas inverted parabolic thermal gradient is most unstable and PLHB is most unstable whereas SF is most stable.

The influence of inter-phase thermal diffusivity ratio τ over critical Rayleigh number are depicted in figures 5.1 and 5.2 when $\tau = 0.1$, 0.5 and 1. The curves diverge and hence the composite layer where $d_m \gg d$ is best suited for the influence of this parameter. Also, critical Rayleigh number decreases when there is increase in τ thereby destabilizing the system. Hence, quicker onset of DRBMM convection is observed.

The effects of α_{FTE}, fluid phase thermal expansion ratio on the critical Rayleigh number are depicted through figures-6.1 and 6.2. The curves are diverging with assigned values $\alpha_{FTE} = 1$, 5 and 10 which proves that variation effect is dilating in a composite sysem where $d \ll d_m$. It is also evident from the figure that increase in α_{FTE} results into decrease in critical Rayleigh number and hence the set-up can be destabilized. The control of DRBMM convection effusively dependent on the thermal expansion of the fluid phase with respect to all the six gradients. Lesser the thermal expansion of the fluid phase, better is the control of DRBMM convection.

The influence of fluid phase thermal diffusivity ratio κ_{FTD} over critical Rayleigh number are displayed in figures-7.1 and 7.2 fixing κ_{FTD} at 0.1, 0.4 and 0.7. The curves are found diverging showing that it is sensitive when composite layer is dominated by porous layer. The system is destabilized theeby supporting early

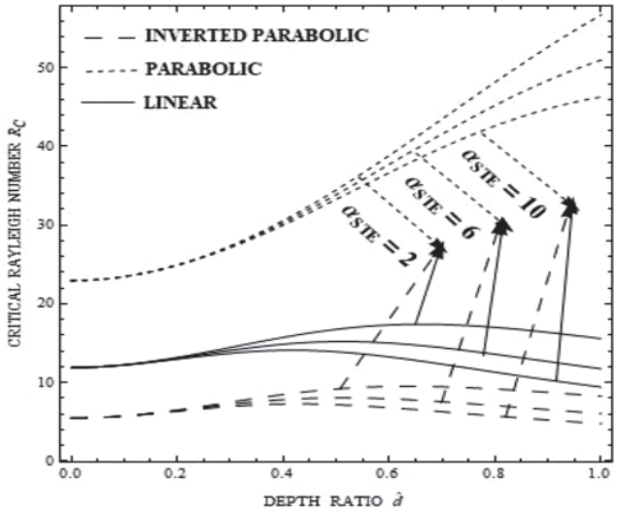

Figure 3.1

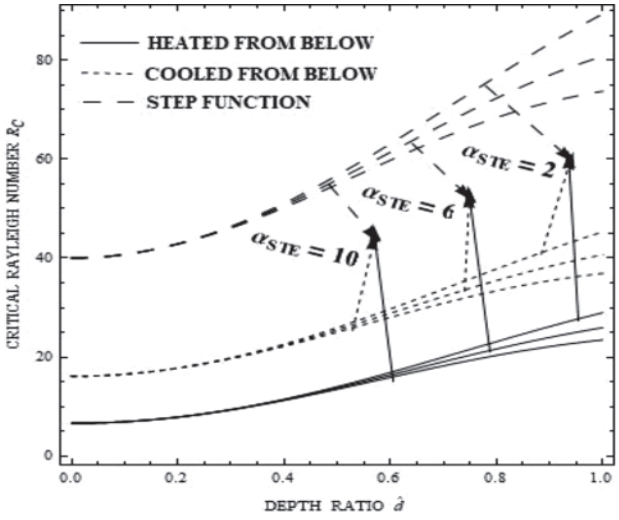

Figure 3.2

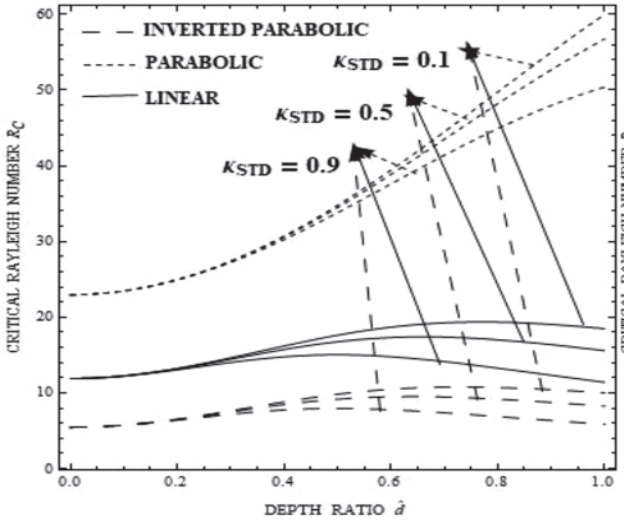

Figure 4.1

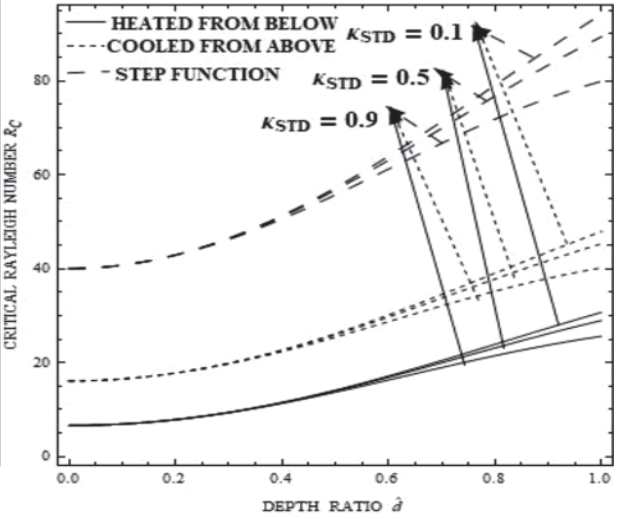

Figure 4.2

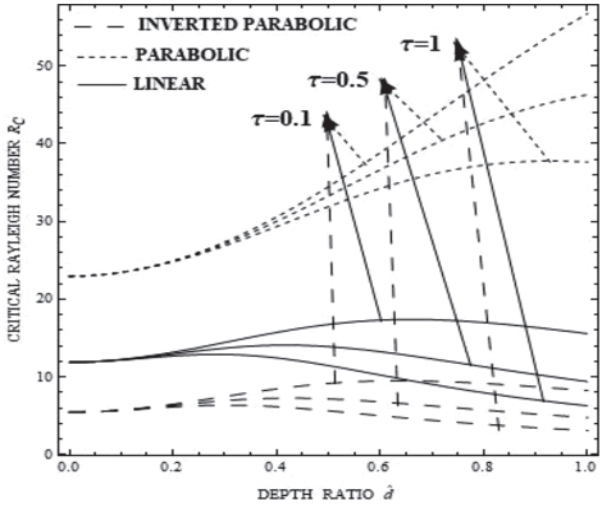

Figure 5.1

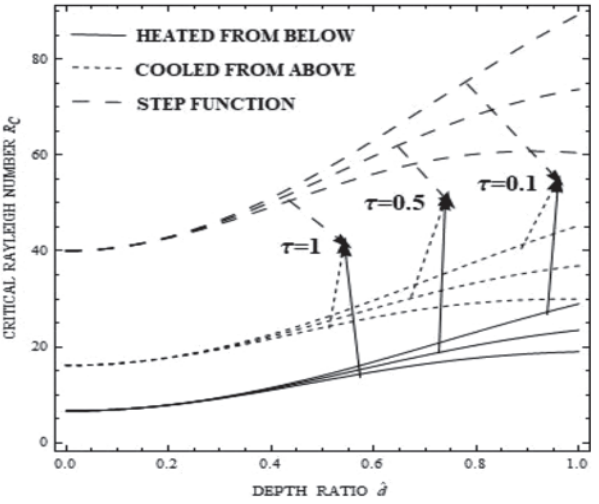

Figure 5.2

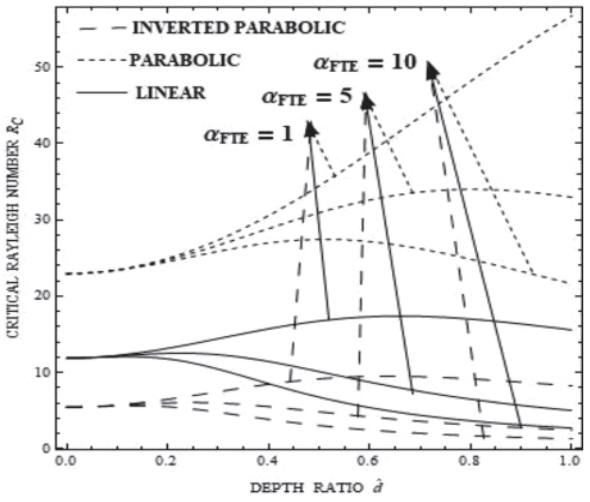

Figure 6.1

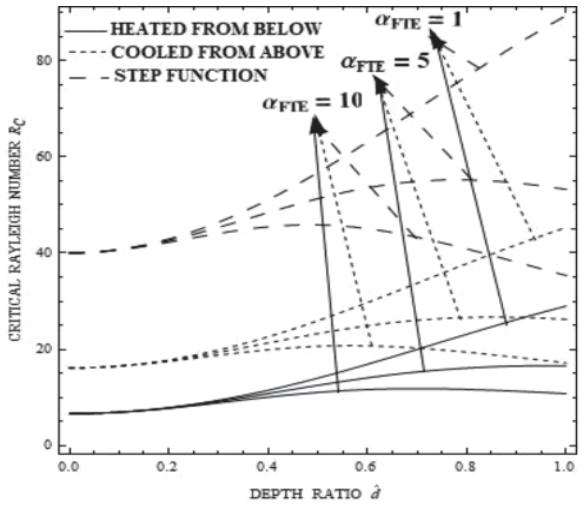

Figure 6.2

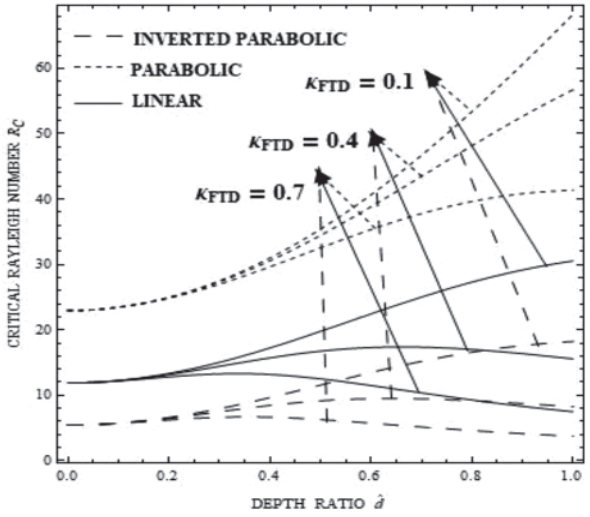

Figure 7.1

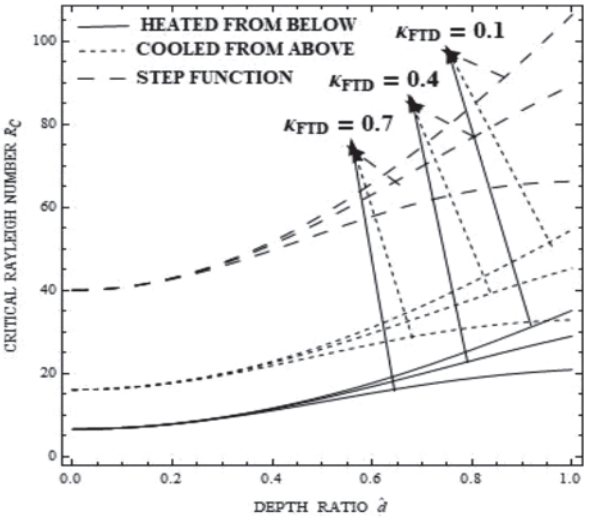

Figure 7.2

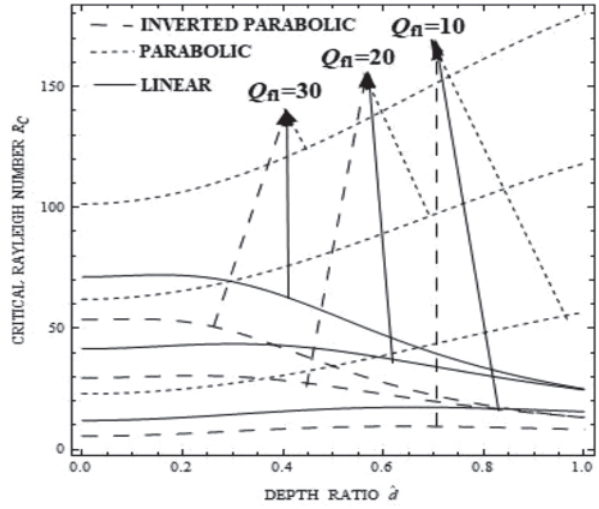

Figure 8.1

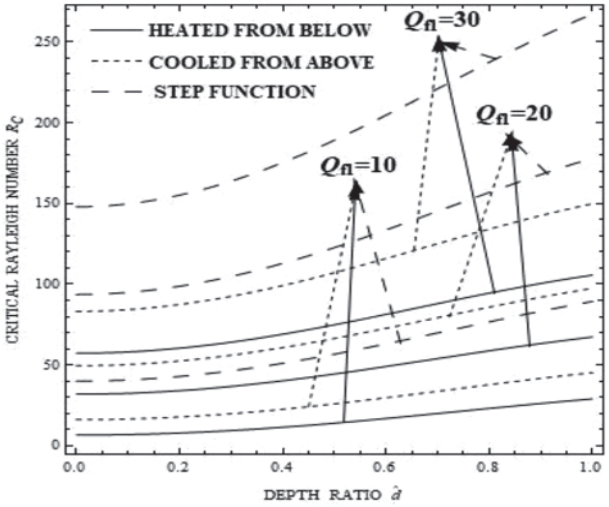

Figure 8.2

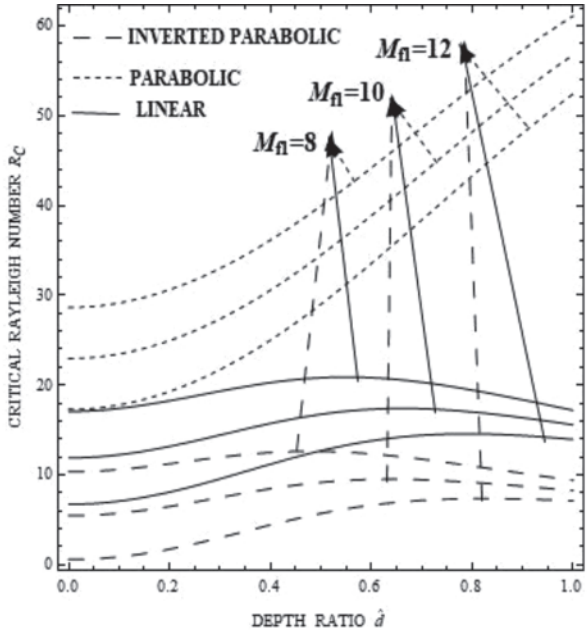

Figure 9.1

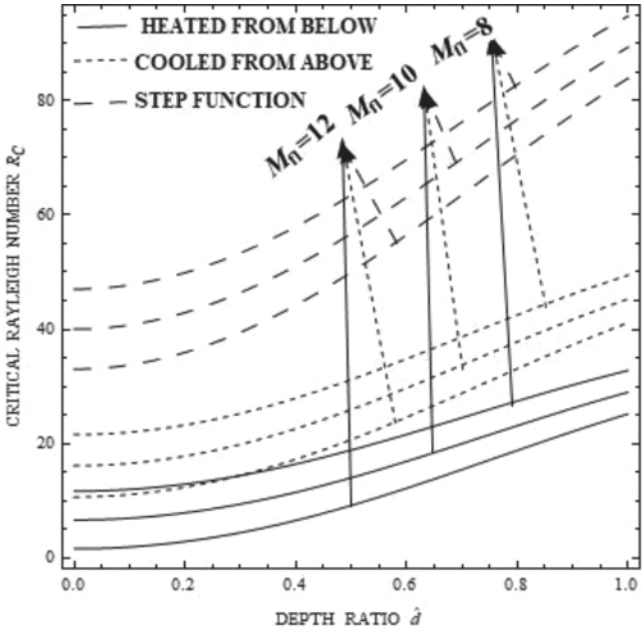

Figure 9.2

onset of DRBMM Convection. Lower values of thermal diffusivity of fluid phase plays a vital role in controllng the DRBMM convection.

The influence of Chandrasekhar number Q_{fl} over critical Rayleigh number are represented in figures 8.1 and 8.2 for Q_{fl} = 10, 20, 30. In this case the curves are converging for higher values of Q_{fl} in case of linear and inverted parabolic thermal gradients indicating that it is sensitive for fluid layer dominant composite layer for these two gradients. The impact of this parameter with respect to the remaining four thermal gradients is found to be well balanced throughout the composite layer. Here, Increase in the parameter rises the critical Rayleigh number thereby stabilizing the system resulting in postponement of DRBMM convection.

The effects of Marangoni number M_{fl} over critical Rayleigh number are displayed in figures-9.1 and 9.2. Slight convergence of the curves is noticed in case of linear and inverted parabolic thermal gradients for values of M_{fl} = 8, 10 and 12. Hence the effect becomes prominent in the composite system dominated by fluid layer for these two profiles and neutral with respect to all the four remaining gradients.

Conclusions

The following conclusions are drawn from the above investigation.

i. For $0<\hat{d}<0.6$ we have
$R_{CIP}<R_{CBEB}<R_{CL}<R_{CCFA}<R_{CP}<R_{CSF}$ and
For $\hat{d}>0.6$ we have
$R_{CIP}<R_{CL}<R_{CHFB}<R_{CCFA}<R_{CP}<R_{CSF}$

ii. Lower values of the parameters viz. fluid phase thermal expansion ratio, solid phase thermal expansion ratio, fluid phase thermal diffusivity ratio and solid phase thermal diffusivity ratio are desirable to control DRBMM convection.

iii. Chandrasekhar number delays the onset of DRBMM covection and the effect of this parameter is protruding in case of linear and inverted parabolic thermal gradients when the composite system is dominated by fluid layer. The effect of magnetic field is to stabilize the system.

iv. Marangoni number boosts the quicker onset of DRBMM convection and the effect of this parameter is prominent with respect to linear and inverted parabolic thermal gradients in fluid dominant composite layer.

References

[1] Armaghani T, M. J. Maghrebi, A. J. Chamkha, and A. F. Al-Mudhaf , Forced Convection Heat Transfer of Nanofluids in a Channel Filled with Porous Media Under Local Thermal Non-Equilibrium Condition with Three New Models for Absorbed Heat Flux, Journal of Nanofluids Vol. 6, pp. 362–367, doi:10.1166/jon.2017.1323, 2017.

[2] Ashoka S. B, A New Algorithm Based SLM to Find Critical Eigenvalue in the Rayleigh-Bénard-Brinkman Convection Problem with Boundary Conditions, Advances in Computational Sciences and Technology ISSN 0973-6107 Volume 10, Number 6 (2017) pp. 1557-1570.

[3] Barbosa J. R., Jr, Two-phase non-equilibrium models: the challenge of improving phase change heat transfer prediction, J. Braz. Soc. Mech. Sci. & Eng. 27 (1) • Mar 2005 • https://doi.org/10.1590/S1678-58782005000100003.

[4] Israa M. Mankhi and Shatha A. Haddad, Effect of local thermal non-equilibrium on the onset of convection in an anisotropic bidispersive porous layer, Journal of Al-Qadisiyah for Computer Science and Mathematics Vol. 13(2) 2021 , pp Math . 181–192.

[5] Min Zeng and Qiuwang Wang, Natural convection of diamagnetic fluid in an enclosure filled with porous medium under magnetic field, Progress in Computational Fluid Dynamics, Vol. 9, No. 2, 2009.

[6] Mohsen Izadi, Rasul Mohebbi, Amin Amiri Delouei and Hasan Sajjadi, Natural convection of a magnetizable hybrid nanofluid inside a porous enclosure subjected to two variable magnetic fields, International Journal of Mechanical Sciences 151 (2019) 154–169.

[7] Noura Alsedais, Abdelraheem M. Aly and Mohamed Ahmed Mansour, Local thermal non-equilibrium condition on mixed convection of a nanofluid-filled undulating cavity containing obstacle and saturated by porous media, Ain Shams Engineering Journal, Volume 13, Issue 2, March 2022, 101562

[8] Sridhar Kulkarni, Unsteady Thermal Convection In A Rotating Anisotropic Porous Layer Using Thermal Non-Equilibrium Model, International Journal of Physics and Mathematical Sciences ISSN: 2277-2111 (Online) An Online International Journal Available at http://www.cibtech.org/jpms.htm 2013 Vol. 3 (3) July-September, pp.30-46/Kulkarni.

[9] Sumithra R and N. Manjunatha, Effects of Heat Source/ Sink and non-uniform temperature gradients on Darcian-Benard-Magneto-Marangoni convection in ‘ composite layer horizontally enclosed by adiabatic boundaries, Malaya Journal of Matematik, Vol. 8, No. 2, 373-382, 2020 https://doi.org/10.26637/MJM0802/0010.

[10] Sumithra R, Manjunatha N and Komala B, Non-Darcian-Benard-magneto-surface tension driven convection in an infinite horizontal composite layer in the presence of heat source/sink and non-uniform temperature gradients, Malaysian Journal of Fundamental and Applied Sciences Vol. 16, No. 6 (2020) 615-624,